Available online at www.sciencedirect.com
SCIENCE DIRECT®
Journal of Sound and Vibration 285 (2005) 1093–1107
JOURNAL OF SOUND AND VIBRATION
www.elsevier.com/locate/jsvi

The effect of temperature on the large amplitude vibrations of curved beams

Pedro Ribeiro[a,*], Emil Manoach[b]

[a]*IDMEC/DEMEGI, Faculdade de Engenharia, Universidade do Porto, Rua Dr. Roberto Frias, 4200-465 Porto, Portugal*
[b]*Institute of Mechanics, Bulgarian Academy of Sciences, Acad G. Bonchev Street, Block 4, 1113 Sofia, Bulgaria*

Received 7 November 2003; received in revised form 6 September 2004; accepted 15 September 2004
Available online 2 December 2004

Abstract

The thermoelastic, geometrically nonlinear vibrations of isotropic, straight and curved beams are studied using *p*-version, hierarchical finite elements. First-order shear deformation theory is followed, and both the longitudinal displacements and inertia are taken into account. The nonlinear equations of motion are solved in the time domain by Newmark's method. The influence of parameters like the temperature variation, the thickness and the ratio of curvature on the beams nonlinear dynamics is studied. Periodic and non-periodic motions are found.
© 2004 Elsevier Ltd. All rights reserved.

1. Introduction

Large amplitude vibrations introduce a geometrical type of nonlinearity that influences the dynamic behaviour of a structure. In fact, the structure's stiffness, and consequently the resonance frequencies and mode shapes, are amplitude dependent [1]. It is also well known that temperature variations from a reference temperature may cause quite significant changes in the dynamic behaviour of a structure, as temperature fields introduce stresses due to thermal expansion or contraction, and can cause buckling of structures with fixed ends [2]. Therefore, the problem of

*Corresponding author. Tel: +351 22 508 17 13; Fax: +351 22 508 14 45.
E-mail address: pmleal@fe.up.pt (P. Ribeiro).

0022-460X/$ - see front matter © 2004 Elsevier Ltd. All rights reserved.
doi:10.1016/j.jsv.2004.09.010

geometrically nonlinear vibration with temperature effects is an interesting one, with wide applicability in engineering.

Beams, straight or curved, are fundamental elements in machines and structures, and one can find several publications devoted to the study of their linear and nonlinear vibrations. As far as the linear vibrations of curved beams are concerned, one of the main motives of research is the alleviation of the shear locking phenomenon in finite elements [3,4]. The nonlinear vibration of curved beams is a particularly interesting problem, which has been investigated, for example, in Refs. [5–7]. In the first Ref. [5], a two-mode model was applied, which has the advantage of being small, but might not be accurate enough for some investigations. In Ref. [6], nonlinear steady-state vibration of beams, frames and shallow arches were analysed in the frequency domain, using a *h*-version straight beam finite element. Undamped, free vibrations of curved Timoshenko beams were analysed in [7] by the Galerkin method, which was applied both in the space and time domains. In these references the temperature effects were not considered.

Although the temperature and elastic behaviours are in fact coupled [2,8], for thin structures—beams, plates or shells—it is often reasonable to assume that the temperature distribution is independent from the deformation of the structure. This gives rise to uncoupled problems, which were investigated, for example, in [9–15]. Chang et al. [9] performed an analytical analysis of heated plates using one term Galerkin approximation and Berger's simplified theory. Locke [10] studied the large deflection of thin, in the Kirchhoff sense, laminated composite plates subjected to static, temperature and acoustic loads. A single mode Galerkin approximation was followed. In [11] a finite element method (FEM) for large amplitude oscillation of panels with the influence of temperature is presented. In [12] a FEM time domain modal formulation for the nonlinear flutter of panels at elevated temperatures is introduced. Limit-cycle and chaotic oscillations are found. A preliminary given distribution of the temperature field is accepted as well in [13], where geometrically nonlinear vibrations of thermally buckled slender panels are investigated using a FE model. In [14] governing equations for geometrically nonlinear vibrations of shells under linear and parabolic temperature distributions are derived. The equations are solved assuming that the deflection is given by one term and applying Galerkin's method. In [15], a formulation based on the FEM and modal analysis is applied to analyse thermal post-buckling of thin simply supported plates.

In the *p*-version of the FEM, the accuracy of the approximation is improved by increasing the number of shape functions over the elements. Several works demonstrate that, in general, the *p*-version of the FEM gives accurate results with fewer degrees of freedom than the *h*-version, which is a big advantage in nonlinear analysis [1,16,17]. Moreover, *p*-elements are not prone to shear locking [17] and, if orthogonal shape functions are chosen, the linear matrices are diagonal. A *p*-version of the FEM where the set of functions corresponding to an approximation of lower order p, constitutes a subset of the set of functions corresponding to the approximation of order $p+1$, is called the ''hierarchical finite element method'' (HFEM) [16]. This has additional advantages, like the fact that linear matrices of different orders of approximation are embedded.

An analysis of the current state of the art in thermoelastic geometrically nonlinear vibrations of structures reveals that the highly efficient *p*-version, hierarchical FEM has not been used to study this problem. In the following pages, a *p*-version, hierarchical finite element for isotropic, linear elastic, curved beams is applied to study thermoelastic geometrically nonlinear vibrations. First-order shear deformation theory is followed; the longitudinal displacements and the longitudinal

inertia are not neglected. The nonlinear equations of motion are solved in the time domain. The influence on the beam nonlinear dynamics of parameters like the temperature variation, the thickness and the ratio of curvature are investigated.

2. Finite element model

A curved beam of thickness h, whose undeformed geometry is defined from a reference straight line by introducing a curvature radius R, is considered. Therefore, the centroidal axis is initially located at a distance from the x-axis given by

$$w^i(x) = -\frac{1}{2}\left(\frac{x^2}{R}\right). \tag{1}$$

The axial displacement, u, is a function of the longitudinal displacement along the centroidal axis u^0 and of the rotation about the y-axis, which is denoted by θ_y^0. The superscript "0" represents the centroidal axis and the rotations follow the right-hand rule. Using a first-order shear deformation model, the displacements are given by

$$u(x,z,t) = u^0(x,t) + z\theta_y^0(x,t), \tag{2}$$

$$w(x,z,t) = w^0(x,t) + w^i(x), \tag{3}$$

where w is the displacement along the z direction and w^0 is the deformation in relation to the initial configuration. The longitudinal strains of curved beams are given by

$$\varepsilon_x = \begin{bmatrix} 1 & z \end{bmatrix}\left(\begin{Bmatrix} \varepsilon_0^p \\ \varepsilon_0^b \end{Bmatrix} + \begin{Bmatrix} \varepsilon_I \\ 0 \end{Bmatrix} + \begin{Bmatrix} \varepsilon_L^p \\ 0 \end{Bmatrix}\right), \tag{4}$$

where the linear longitudinal and bending strains, ε_0^p and ε_0^b, and the geometrically nonlinear longitudinal strain, ε_L^p, are defined as

$$\varepsilon_0^p = u_{,x}^0, \quad \varepsilon_0^b = \theta_{y,x}^0, \quad \varepsilon_L^p = \frac{(w_{,x}^0)^2}{2}. \tag{5}$$

The following strain is due to the initial curvature of the arch and to the transverse displacement:

$$\varepsilon_I = \frac{w^0}{R}. \tag{6}$$

The transverse shear strain is

$$\gamma_{zx}^0 = w_{,x}^0 + \theta_y^0. \tag{7}$$

The other strains are zero. Naturally, the strains and displacements in Eqs. (4)–(7) depend on the position x and on time t, but in order to simplify the notation $\varepsilon_x(x,t)$ is represented as ε_x, etc.

When a beam is heated and the temperature distribution is uniform, its dimensions tend to change due to a thermal deformation that can be expressed as $\varepsilon_T = \alpha(T - T_{\text{ref}}) = \alpha\Delta T$. The letter T represents the actual temperature, and T_{ref} is a reference temperature for zero thermal strain. If the beam is constrained by boundary conditions that do not allow an axial deformation to occur,

then an axial compressive stress will result and the following stress–strain relation holds:

$$\sigma_x = E(\varepsilon_0^p + \varepsilon_L^p + \varepsilon_I - \varepsilon_T - z\kappa_x). \tag{8}$$

The relation between the average shear stress and the shear strain is the usual

$$\tau_{xz} = \lambda G \gamma_{xz}. \tag{9}$$

In the former equations, E represents the modulus of elasticity and G is the shear modulus of elasticity, given by $E/(2(1+\nu))$, where ν is the Poisson ratio. The shear correction factor, λ, depends on the beam's cross-section, and different values have been suggested. According to [18], the expression $\lambda = (5+5\nu)/(6+5\nu)$, which will be used in this paper, gives an appropriate value for rectangular beams. Material properties, like E, G and α, may vary appreciably when the temperature changes a few hundred degrees [2], but in this work the temperature changes will be moderate, and constant material properties will be assumed.

In the FEM, the middle surface elemental displacements are expressed in the form:

$$\begin{Bmatrix} u^0 \\ w^0 \\ \theta_y^0 \end{Bmatrix} = \begin{bmatrix} \{N^u\}^{\mathrm{T}} & 0 & 0 \\ 0 & \{N^w\}^{\mathrm{T}} & 0 \\ 0 & 0 & \{N^{\theta_y}\}^{\mathrm{T}} \end{bmatrix} \begin{Bmatrix} q_u \\ q_w \\ q_{\theta_y} \end{Bmatrix}, \tag{10}$$

where $\{q_u\}$ is the vector of generalised longitudinal displacements, $\{q_w\}$ is the vector of generalised transverse displacements, and $\{q_{\theta_y}\}$ is the vector of generalised rotations. The complete matrix of shape functions is constituted by the row vectors of longitudinal, transverse and rotational shape functions, which are, respectively, $\{N^u\}^{\mathrm{T}}$, $\{N^w\}^{\mathrm{T}}$ and $\{N^{\theta_y}\}^{\mathrm{T}}$. In the HFEM the number of shape functions can vary as deemed necessary by the user. The sets of shape functions used here are given in [1].

The stress and couple resultants and the shear stress resultant per unit length are, respectively, defined by $T_x = \int_{-h/2}^{h/2} \sigma_x \, \mathrm{d}z$, $M = \int_{-h/2}^{h/2} \sigma_x z \, \mathrm{d}z$ and $Q_z = \int_{-h/2}^{h/2} \tau_{xz} \, \mathrm{d}z$. Substituting the stresses by their relations with the strains, Eqs. (8) and (9), one arrives at the thermoelastic constitutive relations of the curved beam. Because beams of symmetric cross section are considered, there are no coupling terms between extension and bending and the following relation holds:

$$\begin{Bmatrix} T \\ M \end{Bmatrix} = \begin{bmatrix} A & 0 \\ 0 & D \end{bmatrix} \left(\begin{Bmatrix} \varepsilon_0^p \\ \varepsilon_0^b \end{Bmatrix} + \begin{Bmatrix} \varepsilon_L^p \\ 0 \end{Bmatrix} + \begin{Bmatrix} \varepsilon_I \\ 0 \end{Bmatrix} - \begin{Bmatrix} \varepsilon_T \\ 0 \end{Bmatrix} \right), \tag{11}$$

$$Q_x = \lambda G h \gamma_{xz} \tag{12}$$

with

$$A = Eh, \quad D = \frac{Eh^3}{12}.$$

The equations of motion are derived by equating the sum of the virtual work of the inertia forces and of the elastic restoring forces to zero. The virtual work of the internal forces is

$$\delta W_{\text{in}} = -b\int_L \left(\begin{Bmatrix} \delta\varepsilon_0^p \\ \delta\varepsilon_0^b \end{Bmatrix}^{\mathrm{T}} + \begin{Bmatrix} \delta\varepsilon_I \\ 0 \end{Bmatrix}^{\mathrm{T}} + \begin{Bmatrix} \delta\varepsilon_L^p \\ 0 \end{Bmatrix}^{\mathrm{T}} \right) \begin{bmatrix} A & 0 \\ 0 & D \end{bmatrix} \times \left(\begin{Bmatrix} \varepsilon_0^p \\ \varepsilon_0^b \end{Bmatrix} + \begin{Bmatrix} \varepsilon_L^p \\ 0 \end{Bmatrix} + \begin{Bmatrix} \varepsilon_I \\ 0 \end{Bmatrix} - \begin{Bmatrix} \varepsilon_T \\ 0 \end{Bmatrix} \right) \mathrm{d}x - b\int_L \delta\gamma_{zx}\lambda G h \gamma_{zx}\,\mathrm{d}x. \tag{13}$$

The linear stiffness matrices are defined from the products involving only linear strains. These are: the longitudinal stiffness matrix $[K_1^p]$, which is equal to the straight beam one [1]; the bending matrix $[K_1^b]$; the matrices due to coupling between the transverse response and the longitudinal response $[K_1^b]$ and $[K_1^{ps}]$ and the matrix $[K_1^{ss}]$, due to the beam's initial curvature. The former matrices and the linear shear stiffness matrix $[K_1^\gamma]$ are given in Appendix A.

There are three nonlinear stiffness matrices—$[K_2]$, $[K_3]$ and $[K_4]$—which are functions of the transverse generalised displacements $\{q_w\}$, and are equal to the thin straight beam ones [1]. Two nonlinear stiffness matrices due to the beams' initial curvature also appear. These are matrix $[K_2^s]$, given in Appendix A, and matrix $[K_3^s] = 2[K_2^s]^{\mathrm{T}}$. The integrals that appear in the calculation of these matrices are computed symbolically only once for each model, and stored in a file in Fortran format. These matrices are updated in each iteration.

The temperature variations originate two force vectors. One is the vector of longitudinal thermal forces, which for beams of constant cross section is

$$\{F_{Tu}\} = bA\alpha\Delta T\int_L \left\{N_{,x}^u\right\}\mathrm{d}x. \tag{14}$$

The other is a vector of thermal forces in the transverse direction, which appears due to the beam's initial curvature and to the thermal expansion. This vector is given by

$$\{F_{TS}\} = \frac{bA\alpha\Delta T}{R}\int_L \{N^w\}\,\mathrm{d}x. \tag{15}$$

The two former expressions are valid as long as neither ΔT, nor A depend on the longitudinal coordinate x.

The nonlinear deformation and the thermal strain generate the following matrix:

$$[K^{\Delta T}] = bA\alpha\Delta T\int_L \left\{N_{,x}^w\right\}\left\{N_{,x}^w\right\}^{\mathrm{T}}\mathrm{d}x. \tag{16}$$

The virtual work of the inertia forces is

$$\delta W_j = -b\int_{-h/2}^{h/2}\int_L \rho(\delta u\,\ddot{u} + \delta w\,\ddot{w})\,\mathrm{d}x\,\mathrm{d}z. \tag{17}$$

Hence, the mass matrix $[M]$ will include the sub-matrices $[M_p]$ and $[M_b]$, which are the longitudinal and transverse inertia matrices, and the sub-matrix $[M_R]$, which is due to the rotatory inertia. In this work none of these matrices is neglected.

The principle of the virtual work is applied to compute the vector of generalised forces due to external mechanical actions. Considering as an example the point load, $P_j^w(t)$, and the distributed transverse load, $P_d^w(x,t)$, the following expression applies:

$$\delta W_{\text{ex}} = \int_L \left[P_j^w(t)\delta(x-x_j) + P_d^w\right]\delta w(x,t)\,\mathrm{d}L$$

$$\Leftrightarrow \quad \delta W_{\text{ex}} = \left\{0 \quad \delta q_w \quad 0\right\}^{\mathrm{T}} \begin{Bmatrix} 0 \\ F_w^E \\ 0 \end{Bmatrix}, \tag{18}$$

where $\delta(x-x_j)$ represents a spatial Dirac delta function. A similar procedure is followed to obtain the vectors of generalised externally applied longitudinal forces $\{F_u^E\}$ and moments $\{M^E\}$.

For simplicity's sake, stiffness proportional damping will be assumed, and the following time domain equations of motion in generalised coordinates are obtained:

$$\begin{bmatrix} [M_p] & 0 & 0 \\ 0 & [M_b] & 0 \\ 0 & 0 & [M_R] \end{bmatrix} \begin{Bmatrix} \ddot{q}_u \\ \ddot{q}_w \\ \ddot{q}_{\theta_y} \end{Bmatrix} + \begin{bmatrix} [K_1^p] & [K_1^{ps}] & 0 \\ [K_1^{sp}] & [K_1^{ss}] + [K_1^{\gamma 11}] & [K_1^{\gamma 12}] \\ 0 & [K_1^{\gamma 21}] & [K_1^b] + [K_1^{\gamma 22}] \end{bmatrix} \begin{Bmatrix} q_u \\ q_w \\ q_{\theta_y} \end{Bmatrix}$$

$$+ c \begin{bmatrix} [K_1^p] & [K_1^{ps}] & 0 \\ [K_1^{sp}] & [K_1^{ss}] + [K_1^{\gamma 11}] & [K_1^{\gamma 12}] \\ 0 & [K_1^{\gamma 21}] & [K_1^b] + [K_1^{\gamma 22}] \end{bmatrix} \begin{Bmatrix} \dot{q}_u \\ \dot{q}_w \\ \dot{q}_{\theta_y} \end{Bmatrix}$$

$$+ \begin{bmatrix} 0 & [K_2] & 0 \\ [K_3] & [K_4] + [K_2^s] + [K_3^s] - [K^{\Delta T}] & 0 \\ 0 & 0 & 0 \end{bmatrix} \begin{Bmatrix} q_u \\ q_w \\ q_{\theta_y} \end{Bmatrix} = \begin{Bmatrix} F_{Tu} \\ F_{TS} \\ 0 \end{Bmatrix} + \begin{Bmatrix} F_u^E \\ F_w^E \\ M^E \end{Bmatrix}. \tag{19}$$

3. Numerical studies and discussions

All beams analysed are in aluminium with elasticity modulus $E = 7 \times 10^{10}\,\mathrm{N/m^2}$, mass density $\rho = 2778\,\mathrm{kg/m^3}$, and Poisson coefficient $v = 0.34$. The thermal expansion coefficient is $\alpha = 23.90 \times 10^{-6}/\mathrm{K}$ and the shear correction factor is, as already stated, $\lambda = (5+5v)/(6+5v)$. In the first series of examples it will be assumed that the damping coefficient is $c = 10^{-3}$; afterwards, the value $c = 10^{-4}$ will be employed. Only one hierarchical finite element is used to model each beam. The boundaries are clamped–clamped.

First, a straight beam with the following geometric properties is analysed: $b = 0.02\,\mathrm{m}$, $h = 0.002\,\mathrm{m}$, $L = 0.5\,\mathrm{m}$. Using a finite element with 9 transverse shape functions, 9 longitudinal

shape functions and 9 rotational shape functions, that is, 27 dof, the values calculated for the first four natural frequencies (rad/s) are: 259.338, 714.774, 1401.00, 2315.64. These agree with the analytical results [19].

In Fig. 1, the displacements of the beam's middle point are displayed. The beam is excited at its first natural frequency by a harmonic excitation with 1 N, applied transversely at midspan and different variations in temperature are implemented. When negative variations of temperature are considered, one verifies, as expected, that a straight beam becomes stiffer, and that, therefore, the displacements amplitudes are smaller. On the other hand, as the temperature increases the beam softens, and its vibration amplitudes increase.

With ΔT equal to -5, 0 or 1 K the motions are periodic and symmetric around the corresponding equilibrium position, which is the original straight configuration. For ΔT equal or higher than 4 K, the beam oscillates again with periodic motions, but around a new, buckled, equilibrium configuration.

With this 1 N point excitation, a very interesting motion occurs $\Delta T = 3$ K, as the time, phase and Poincaré plots in Fig. 2 demonstrate. In this far from periodic motion, the beam moves around three equilibrium positions, one unstable and two stable. The two buckled equilibrium positions appear because the critical buckling temperature—determined as approximately $\Delta T = 2.2$ K, employing a Bernoulli–Euler model [2]—was passed. The Poincaré plots, represented in this and in the following pictures, were constructed by sampling the velocity and displacements at periods of the excitation force [20].

In Fig. 3, the time history of the displacement and the phase plot of the middle point of the same straight beam is portrayed, but when $\Delta T = 5$ K and the excitation amplitude is 5 N. The temperature is larger than the critical buckling temperature and the force is quite large, so that the beam should pass through its three equilibrium positions. It is thus interesting to find out that the motion became periodic again.

From this simple examination, we verify that the dynamic behaviour of thin beams suffers important changes with temperature. This brings some difficulties when one carries out experimental analyses of beams with fixed boundaries, in a laboratory without a rigorous temperature control [21].

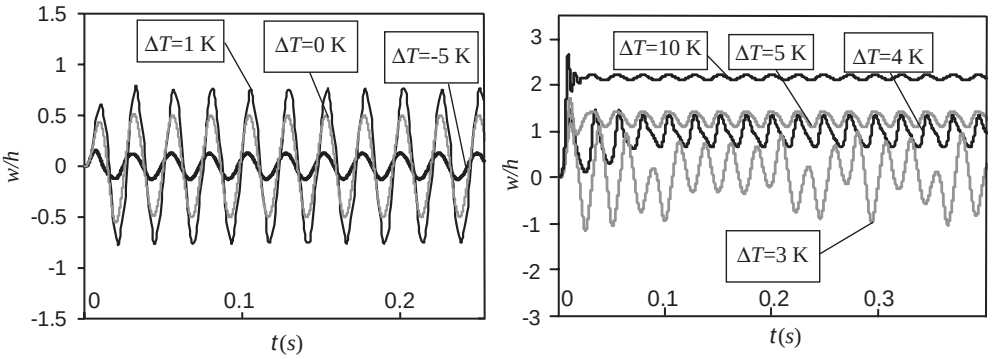

Fig. 1. Time histories of thin straight beam at different temperatures.

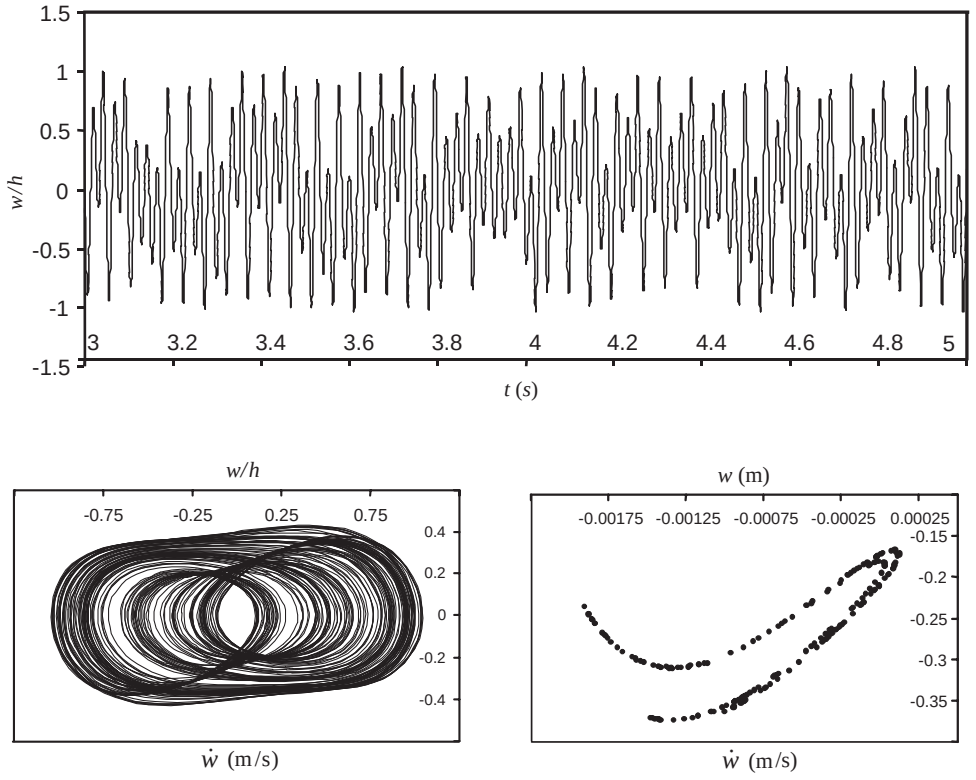

Fig. 2. Time, phase and Poincaré plots of motion of middle point of straight beam, when $\Delta T = 3\,\mathrm{K}$.

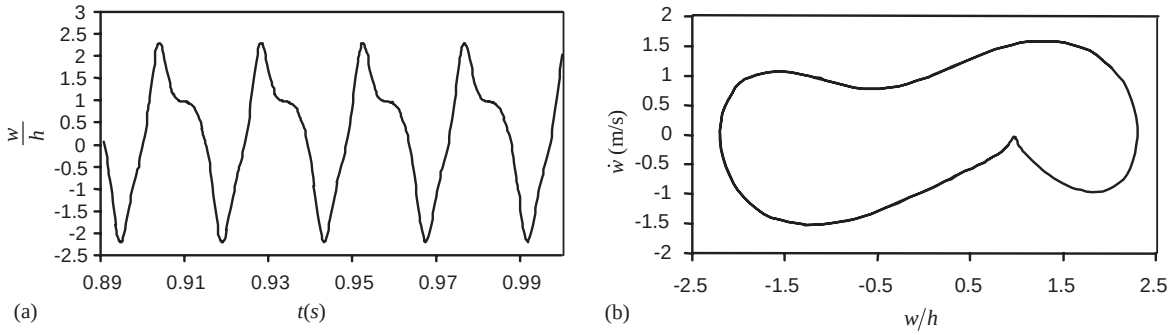

Fig. 3. Time (a) and phase (b) plots representing motion of middle point of straight beam, when $\Delta T = 5\,\mathrm{K}$.

Now, let us study the effects of the beam's thickness by analysing straight beams with the properties previously defined, except the thickness, which will be varied. Two finite elements are applied: the previously used 27 dof element and a hierarchical finite element with 7 shape functions of each type, i.e., 21 dof in total. Compared with the 27 dof element, the 21 dof still

provides very accurate results—if the 5th mode is not important in the motion's definition—with computational time savings. With this 21 dof element, the fourth linear natural frequency is computed with a relative error lower than 0.63%.

Fig. 4 shows the time plots of responses when the excitation frequency is the first natural frequency of the beam under analysis, the temperature variation is either 0 K or 10 K, and the force is distributed with amplitude $50(h/h_1)^3$ N/m, where h_1 is the thickness of the thinner beam ($h_1 = 0.002$ m). The other beams thicknesses are $h_2 = 0.01$ m and $h_3 = 0.02$ m, that is $h_2/L = 0.02$ and $h_3/L = 0.04$.

In spite of the increasing force amplitude, the amplitude of the displacements decreased significantly as the thickness of the beam augmented. Also, as confirmed by the 0 K examples, the thin beam response changes dramatically with the temperature variation, whilst for the medium beam the effects of the temperature are smaller and the thicker beam has a similar response at both temperatures. In fact, at 10 K, the dynamic response to a harmonic excitation changed from a not periodic motion, in the thinner beam case, to a harmonic one in the thicker beams.

By analysing the deformed shapes of the thin beam, it was verified that its motion is affected by higher order modes, in both temperature cases. Nevertheless, these higher modes are much more important when $\Delta T = 10$ K, where the motion is not at all periodic, as the phase and Poincaré plots—Figs. 5 and 6—demonstrate. In this case of non-periodic motions, and because high order

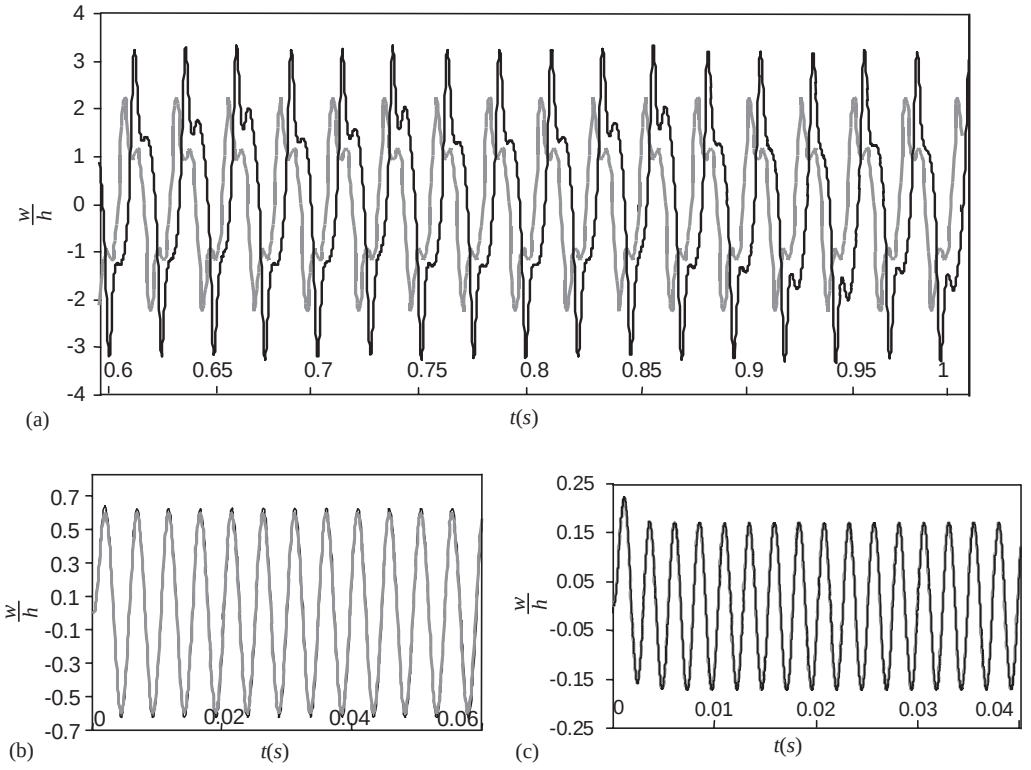

Fig. 4. Time histories of straight beams with different thicknesses. Grey, $\Delta T = 0$ K; black $\Delta T = 10$ K, and (a) $h/L = 0.002$, (b) $h/L = 0.03$, and (c) $h/L = 0.04$.

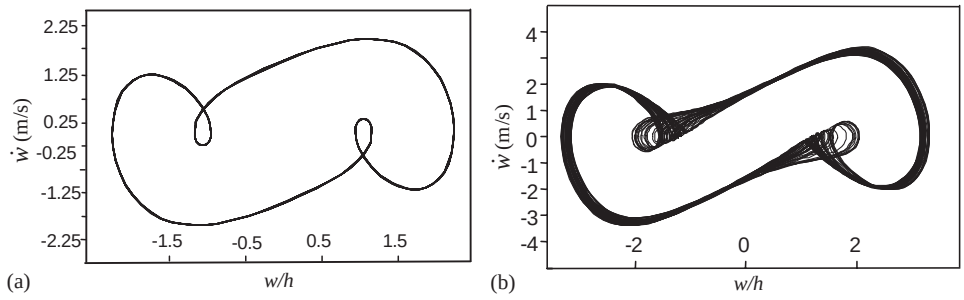

Fig. 5. Phase plots of straight thin beam when $\Delta T = 0\,\mathrm{K}$ (a) and $\Delta T = 10\,\mathrm{K}$ (b).

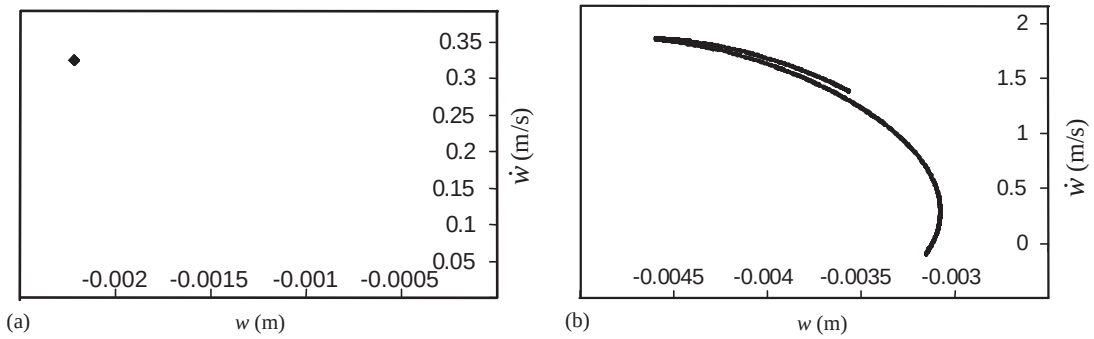

Fig. 6. Poincaré maps of straight thin beam when (a) $\Delta T = 0\,\mathrm{K}$ and (b) $\Delta T = 10\,\mathrm{K}$.

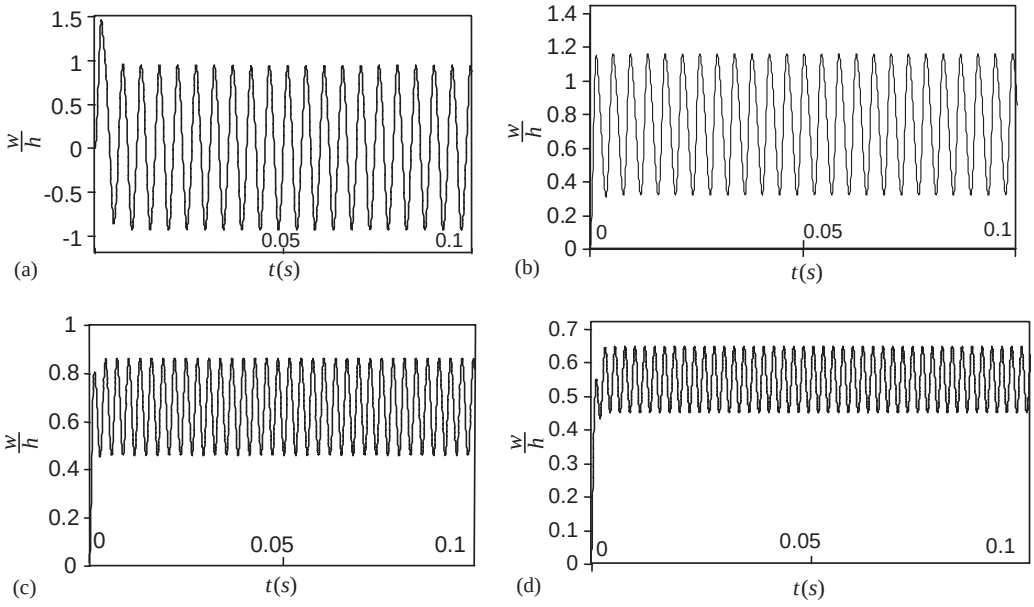

Fig. 7. Time plots for different curved beams ($\Delta T = 100\,\mathrm{K}$): (a) $R = \infty$, (b) $L/R = 0.1$, (c) $L/R = 0.2$, and (d) $L/R = 0.3$.

nonlinear modes are present in the response, slightly different time, Poincaré and phase plots were obtained with the 21 dof and with the 27 dof models. Thus, the results from the more accurate 27 dof model are the ones shown.

In the following examples the thermoelastic vibrations of curved beams, with length $L = 0.5\,\mathrm{m}$ and square cross-section, being $b = h = 0.02\,\mathrm{m}$, are analysed. The 21 dof finite element is used for this purpose.

Let us start by changing the beams' curvature radius, analysing beams where R obeys one of the following relations: $R_1 = \infty$, $L/R_2 = 0.1$, $L/R_3 = 0.2$ and $L/R_4 = 0.3$. The responses of these beams to distributed harmonic excitations with frequency equal to their first natural frequency, and with amplitude 10 kN/m, were computed. The results when the temperature variation is 100 K are shown in Fig. 7.

As the initial curvature radius decreases, the beam becomes stiffer; consequently, the vibration amplitude decreases as L/R increases. However, the transverse thermal force—given by expression (15)—also increases with the curvature of the beam, and, unlike straight beams prior

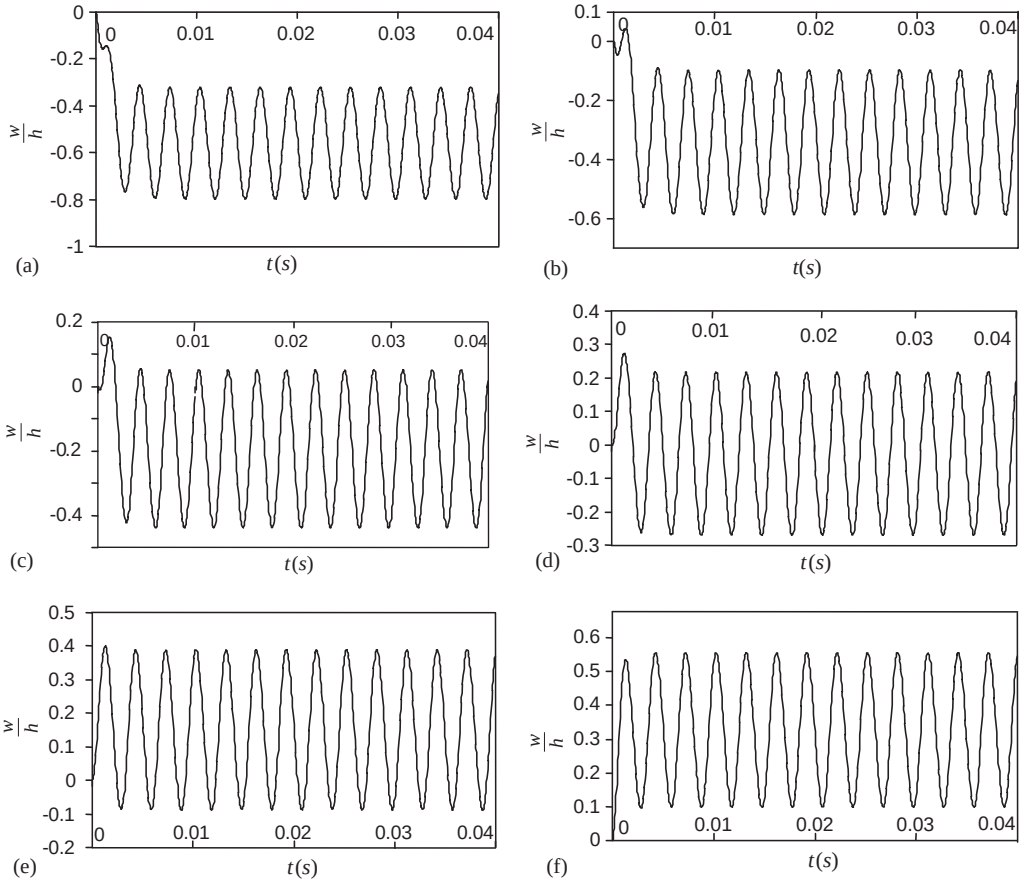

Fig. 8. Time plots for a curved beam under 10 kN/m and different temperature variations: $\Delta T = -100\,\mathrm{K}$ (a), $\Delta T = -50\,\mathrm{K}$ (b), $\Delta T = -25\,\mathrm{K}$ (c), $\Delta T = 0\,\mathrm{K}$ (d), $\Delta T = 25\,\mathrm{K}$ (e), and $\Delta T = 50\,\mathrm{K}$ (f).

to buckling, curved beams always vibrate around an equilibrium position which is displaced relatively to the one of the unheated beam.

Fig. 8 displays the responses of the beam where $L/R = 0.2$, with a mechanical excitation due to a distributed harmonic load with 10 kN/m, but with different temperature changes. In this case, all the motions are periodic, but the temperature variation ΔT alters the equilibrium configuration. For negative temperature variations, the curvature of the beam decreases, and the opposite occurs for positive ΔT.

So far the damping parameter has always been $c = 0.001$. Now, to attain very large amplitude vibrations, this will be reduced to $c = 0.0001$ and the distributed force increased to 40 kN/m. Our goal here is to shown the importance of the curvature in the very large displacement, high temperature, elastic vibrations. One sees in Figs. 9 and 10 that, for this larger excitation force, the motions at the different temperature variations are periodic and do not vary so strongly with the temperature as in other cases. Nevertheless, the amplitudes of vibration and the phase plots

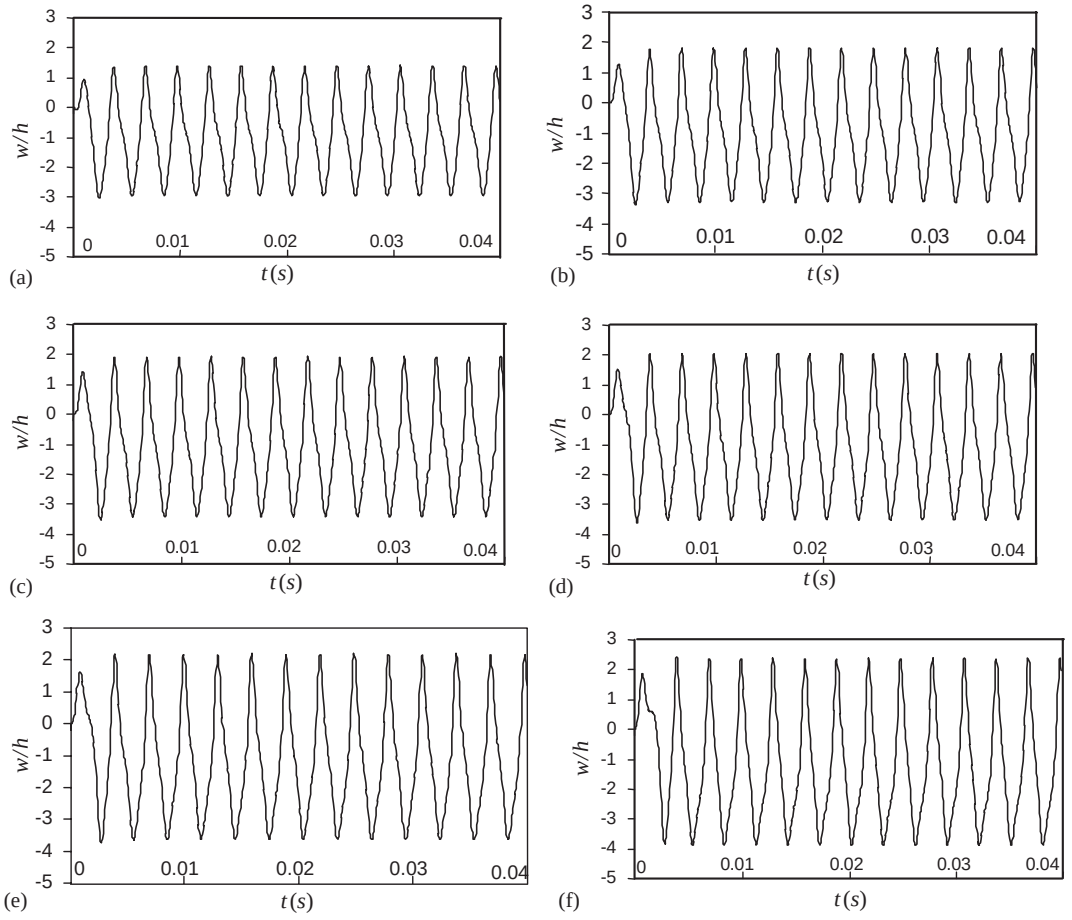

Fig. 9. Time plots for a curved beam under 40 kN/m and different temperature variations: $\Delta T = -100$ K (a), $\Delta T = -25$ K (b), $\Delta T = 0$ K (c), $\Delta T = 25$ K (d), $\Delta T = 50$ K (e), and $\Delta T = 100$ K (f).

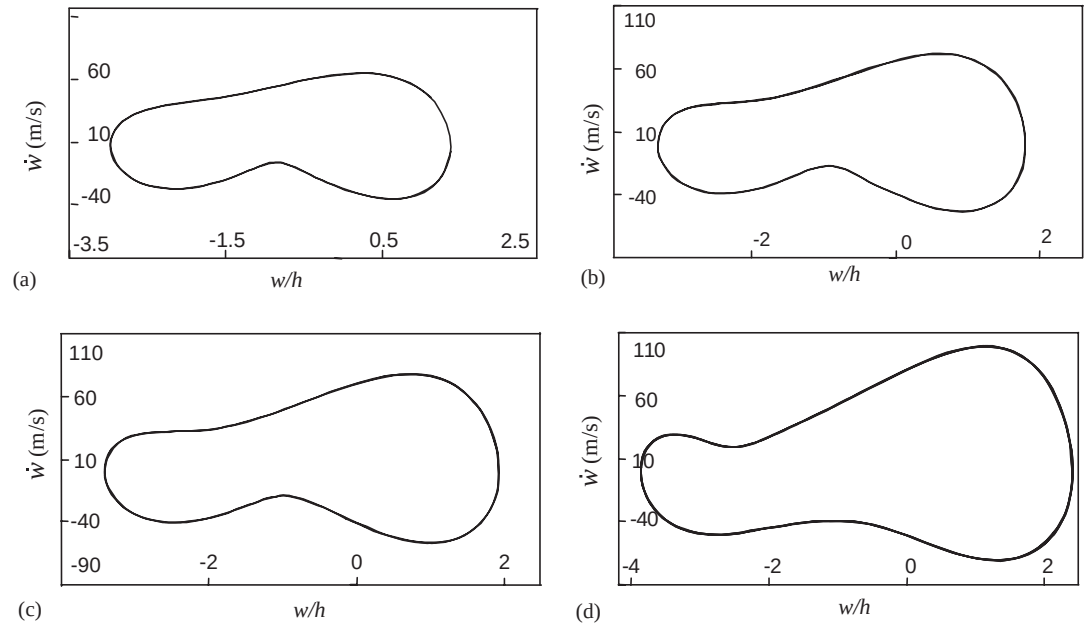

Fig. 10. Phase plots for a curved beam under 40 kN/m and different temperature variations: $\Delta T = -100\,\mathrm{K}$ (a), $\Delta T = -25\,\mathrm{K}$ (b), $\Delta T = 0\,\mathrm{K}$ (c), and $\Delta T = 100\,\mathrm{K}$ (d).

change with the temperature.[1] The non-harmonic response to a harmonic excitation is due to the curvature and nonlinear effects, since it also occurs when $\Delta T = 0\,\mathrm{K}$.

4. Conclusions

The geometrically nonlinear thermoelastic vibrations of straight and curved beams were analysed with a reduced computational cost, using *p*-version, hierarchical finite elements. In the case of straight beams, it was verified that thicker beams are less influenced by temperature variations. On the other hand, thin beams are very sensitive to quite small temperature variations, and may rather easily experience a bifurcation from a motion where there is only one equilibrium configuration, to one where three equilibrium configurations coexist.

Curved beams are influenced in a different way by temperature then straight beams. For positive temperature variations, the curvature and temperature effects result in forces that increase the stiffness and the curvature. On the other hand, if the temperature is reduced, the curvature of the beam tends to decrease. As a result, and unlike straight beams, curved beams always oscillate around an equilibrium position that differs from the equilibrium position at the reference temperature.

Thus, when the temperature increases, strongly non-harmonic and even non-periodic motions are more likely in straight beams that in curved ones. The probable reason behind this is that

[1]For the larger vibration amplitudes shown in the picture, one can doubt if the elastic model employed is still valid.

straight beams with fixed ends easily buckle when they are heated, and therefore they will have one unstable and two stable equilibrium positions. If the mechanical excitation has a large enough amplitude to force the beam to oscillate around these three positions, a rich dynamic behaviour is expected. On the other hand, a heated curved beam will expand and become more curved, and therefore has even more tendency to oscillate around only one equilibrium position. To make this heated curved beam buckle, a larger mechanical external force is required.

Acknowledgments

The authors wish to thank the support of ICCTI/GRICES, Portugal trough the NATO Science fellowship program, as well as the support of the Science and Technology Foundation, Portugal, through grant FEDER POCTI/EME/32641/2000 and of the Bulgarian Research Fund trough grant TH 1103/01.

Appendix A. Stiffness and mass matrices

$$[K_1^b] = bD \int_L \left\{N_{,x}^{\theta_y}\right\}\left\{N_{,x}^{\theta_y}\right\}^{\mathrm{T}} \mathrm{d}x, \tag{A.1}$$

$$[K_1^{ps}] = \frac{bA}{R} \int_L \left\{N_{,x}^{u}\right\}\{N^{w}\}^{\mathrm{T}} \mathrm{d}x, \tag{A.2}$$

$$[K_1^{sp}] = [K_1^{ps}]^{\mathrm{T}}, \tag{A.3}$$

$$[K_1^{ss}] = \frac{bA}{R^2} \int_L \{N^{w}\}\{N^{w}\}^{\mathrm{T}} \mathrm{d}x, \tag{A.4}$$

$$\begin{bmatrix} K_1^{\gamma 11} & K_1^{\gamma 12} \\ K_1^{\gamma 21} & K_1^{\gamma 22} \end{bmatrix} = bG\lambda h \int_L \begin{bmatrix} \left\{N_{,x}^{w}\right\}\left\{N_{,x}^{w}\right\}^{\mathrm{T}} & \left\{N_{,x}^{w}\right\}\left\{N^{\theta_y}\right\}^{\mathrm{T}} \\ \left\{N^{\theta_y}\right\}\left\{N_{,x}^{w}\right\}^{\mathrm{T}} & \left\{N^{\theta_y}\right\}\left\{N^{\theta_y}\right\}^{\mathrm{T}} \end{bmatrix} \mathrm{d}x, \tag{A.5}$$

$$[K_2^s] = \frac{bA}{2R} \int_L \{N^{w}\}\left\{N_{,x}^{w}\right\}^{\mathrm{T}} w_{,x}^{0} \, \mathrm{d}L, \tag{A.6}$$

$$\begin{bmatrix} [M_p] & 0 & 0 \\ 0 & [M_b] & 0 \\ 0 & 0 & [M_R] \end{bmatrix} = \rho h \begin{bmatrix} b\int_L \{N^u\}\{N^u\}^{\mathrm{T}} \mathrm{d}x & 0 & 0 \\ 0 & b\int_L \{N^w\}\{N^w\}^{\mathrm{T}} \mathrm{d}x & 0 \\ 0 & 0 & \frac{1}{12} bh^3 \int_\Omega \left\{N^{\theta_y}\right\}\left\{N^{\theta_y}\right\}^{\mathrm{T}} \mathrm{d}x \end{bmatrix}. \tag{A.7}$$

References

[1] P. Ribeiro, M. Petyt, Non-linear vibration of beams with internal resonance by the hierarchical finite element method, *Journal of Sound and Vibration* 224 (1999) 591–624.

[2] E.A. Thorton, *Thermal Structures for Aerospace Applications*, AIAA Education Series, Reston, VA, 1996.

[3] S.S. Lee, J.S. Koo, J.M. Choi, Development of a new curved beam element with shear effect, *Engineering Computations* 13 (1996) 9–25.

[4] P. Raveendranath, G. Singh, G.V. Rao, A three-noded shear-flexible curved beam element based on coupled displacement field interpolations, *International Journal for Numerical Methods in Engineering* 51 (2001) 85–101.

[5] Q. Bi, H.H. Dai, Analysis of non-linear dynamics and bifurcations of a shallow arch subjected to periodic excitation with internal resonance, *Journal of Sound and Vibration* 233 (2000) 557–571.

[6] S.H. Chen, Y.K. Cheung, H.X. Xing, Nonlinear vibration of plane structures by finite element and incremental harmonic balance method, *Nonlinear Dynamics* 26 (2001) 87–104.

[7] J. Luczko, Bifurcations and internal resonances in space-curved rods, *Computer Methods in Applied Mechanics and Engineering* 191 (2002) 3271–3296.

[8] D. Karagiozova, E. Manoach, Coupling effects in an elastic–plastic beam subjected to heat impact, *Nuclear Engineering and Design* 135 (1992) 267–276.

[9] W.P. Chang, S.C. Jen, Nonlinear free vibrations of heated orthotropic rectangular plates, *International Journal of Solids and Structures* 22 (1986) 267–282.

[10] J. Locke, Nonlinear random response of angle-ply laminates with static and thermal preloads, *AIAA Journal* 29 (1991) 1480–1487.

[11] D.Y. Xue, C. Mei, Finite element nonlinear panel flutter with arbitrary temperatures in supersonic flow, *AIAA Journal* 31 (1993) 154–162.

[12] R.C. Zhou, Y. Xue, C. Mei, Finite element time domain-modal formulation for nonlinear flutter of composite panels, *AIAA Journal* 32 (1994) 2044–2052.

[13] R. Udrescu, Nonlinear vibrations of thermally buckled panels, *Proceedings of Seventh International Conference Recent Advances in Structural Dynamics*, ISVR, Southampton, 2000, pp. 757–768.

[14] U.K. Mandal, P. Biswas, Nonlinear thermal vibrations on elastic shallow spherical shell under linear and parabolic temperature distributions, *Journal of Applied Mechanics* 66 (1999) 814–815.

[15] Y. Shi, R.Y.Y. Lee, C. Mei, Thermal postbuckling of composite plates using the finite element modal coordinate method, *Journal of Thermal Stresses* 22 (1999) 595–614.

[16] L. Meirovitch, H. Baruh, On the inclusion principle for the hierarchical finite element method, *International Journal for Numerical Methods in Engineering* 19 (1983) 281–291.

[17] P. Ribeiro, A *p*-version finite element for non-linear vibration of moderately thick laminated plates, *Proceedings of the 44th AIAA/ASME/ASCE/AHS/ASC Structures, Structural Dynamics, and Materials Conference & Exhibit*, 7–10 April 2003, Norfolk, VA, Paper nr. AIAA 2003-1711.

[18] J.R. Hutchinson, Shear coefficients for Timoshenko beam theory, *Journal of Applied Mechanics* 68 (2001) 87–92.

[19] C.M. Harris, *Shock and Vibration Handbook*, 3rd ed., McGraw-Hill, New York, 1988.

[20] A.H. Nayfeh, B. Balachandran, *Applied Nonlinear Dynamics: Analytical, Computational, and Experimental Methods*, Wiley, New York, 1995.

[21] P. Ribeiro, R. Carneiro, Experimental detection of modal interaction in the non-linear vibration of a hinged–hinged beam, *Journal of Sound and Vibration* 277 (2004) 943–954.